


MRI features of pediatric intracranial germ cell tumor subtypes

Chih-Chun Wu^{1,2}  · Wan-Yuo Guo^{1,2} · Feng-Chi Chang^{1,2} · Chao-Bao Luo^{1,2} · Han-Jui Lee^{1,2} · Yi-Wei Chen^{2,3} · Yi-Yen Lee^{2,4} · Tai-Tong Wong^{5,6}

Received: 10 November 2016 / Accepted: 23 May 2017 / Published online: 27 May 2017
© Springer Science+Business Media New York 2017

Abstract Intracranial germ cell tumors differ in histology and location, and require different clinical management strategies. We characterized the imaging features that may aid pre-operative differentiation of intracranial germinomas and non-germinomatous germ cell tumors (NGGCTs). This retrospective study analyzed 85 patients with intracranial germ cell tumors and adequate preoperative or pretreatment MRIs between 2000 and 2013 at our institution. Pretreatment MRI characteristics, apparent diffusion coefficient (ADC) values, tumor histopathology, and patient outcomes were compared. NGGCTs occurred in the pineal region and cerebral hemispheres more often than germinomas; all bifocal lesions were germinomas. NGGCTs (36.6 ± 17.0 mm) were significantly larger than germinomas (25.7 ± 11.6 mm; $P=0.002$). The presence of pure solid tumor (45.5 vs. 20.0%, $P=0.033$) and an infiltrative margin (20.0 vs. 3.3%, $P=0.035$) were significantly more common in germinomas than NGGCTs. The presence of intratumoral T1 hyperintense foci (66.7 vs. 10.9%, $P<0.001$) and moderate/

marked enhancement (86.7 vs. 50.9%, $P<0.001$) were significantly more common in NGGCTs than in germinomas. Mean ADC_{mean} values ($\times 10^{-3}$ mm²/s) were significantly lower in germinomas (1.113 ± 0.415) than in NGGCTs (2.011 ± 0.694 , $P=0.001$). Combined a lack of T1 hyperintense foci and an ADC_{mean} threshold value (1.143×10^{-3} mm²/s) had the highest specificity (91.3%) and positive predictive value (92.3%), while the combination of lack of a T1 hyperintense foci, no/mild enhancement, and an ADC_{mean} threshold value had 100% sensitivity and 100% negative-predictive value for discriminating germinomas from NGGCTs. Pre-operative conventional MRI characteristics and diffusion-weighted MRI help clinicians to assess patients with intracranial germ cell tumors. Tumor size, location, T1 hyperintense foci, intratumoral cystic components, tumor margin and enhancing patterns demonstrate contrast between germinomas and NGGCTs. Serum tumor markers and adjunctive combination with T1 hyperintensity and/or enhancing pattern with ADC offer potential in preoperative differentiating intracranial germinomas and NGGCTs.

✉ Chih-Chun Wu
ccwu1005@gmail.com

¹ Department of Radiology, Taipei Veterans General Hospital, 201, Section 2, Shih-Pai Road, Taipei 112, Taiwan, ROC

² School of Medicine, National Yang-Ming University, Taipei, Taiwan, ROC

³ Division of Radiation Oncology, Cancer Center, Taipei Veterans General Hospital, Taipei, Taiwan, ROC

⁴ Division of Pediatric Neurosurgery, Neurological Institute, Taipei Veterans General Hospital, Taipei, Taiwan, ROC

⁵ Department of Neurosurgery, Taipei Medical University Hospital, Taipei, Taiwan, ROC

⁶ Taipei Cancer Center, Taipei Medical University, Taipei, Taiwan, ROC

Keywords Apparent diffusion coefficient · Central nervous system · Diffusion-weighted imaging · Germ cell tumor · Magnetic resonance imaging

Introduction

Intracranial germ cell tumors (GCTs) are the third most common type of brain tumor in Asian pediatric patients, after gliomas and medulloblastomas [1–3], although their incidence is much lower in North American and European countries. These tumors comprise a heterogeneous group of neoplasms, broadly classified as germinomas and

non-germinomatous germ cell tumors (NGGCTs) based on clinicopathologic features. NGGCTs include embryonal carcinoma, endodermal sinus tumor (also known as yolk sac tumor), choriocarcinoma, teratoma (immature and mature), and mixed germ cell tumors with more than one element. Although GCTs are highly treatable, with reported 10-year survival rates exceeding 90% [4–6], the overall survival rate for NGGCT is inferior to that of intracranial germinoma, and more extensive surgery combined with radiation therapy and chemotherapy are needed to treat NGGCTs. An appropriate pre-operative diagnosis is required to manage intracranial GCTs appropriately; however, radiographic differentiation between intracranial GCTs and NGGCTs has not yet been fully investigated. A recent study investing ten patients with intracranial germ cell tumors has suggested that apparent diffusion coefficient (ADC) values differed between germinomas and NGGCTs [7]. Here, by reviewing the histopathological and magnetic resonance imaging (MRI) characteristics of intracranial GCTs in a large pediatric population, and the patterns of treatment failure, we sought to achieve an improved preoperative diagnosis and treatment planning, and to elucidate the spreading pattern of intracranial GCTs.

Materials and methods

Patient characteristics

This present retrospective study was approved by the local Institutional Review Board. We retrospectively analyzed the clinical database of Taipei Veterans General Hospital for cases of suspected intracranial germ cell tumors registered from January 1989 to March 2013. Our preliminary search revealed that each case had been treated with different radiation and chemotherapy strategies, while the therapeutic units of radiation also varied. Before 1990, patients received cobalt-based gamma irradiation treatment; from the mid-to-late 1990s, patients received treatment with mega-voltage X-rays using linear accelerators; while, after 2000, patients received treatment with three-dimensional conformal radiotherapy. Thus, to investigate a homogenous patient cohort treated with similar protocols, we restricted our investigations to patients treated at our institution after 2000.

The pathological investigation of intracranial GCTs is often incomplete in many patients, for two reasons. First, stereotactic or endoscopic biopsy—rather than resection of the entire tumor—is performed for most patients, because the high response rates to adjuvant therapies render radical surgery less favorable. However, tumor biopsy has the possibility of misrepresentative tumor considering the frequency of mixed tumor histology within a single GCT.

Second, a diagnosis of intracranial GCT is often possible without a tumor biopsy in patients with elevated tumor markers, such as alpha-fetoprotein and beta-human chorionic gonadotropin. Therefore, our clinical diagnoses were based on levels of serum/CSF tumor markers and adjunctive pathological data when available, with adjunctive MRI appearance. We used detectable elevated serum alpha-fetoprotein (AFP) (>5 ng/dL) and/or β -human chorionic gonadotropin (β -HCG) more than 100 mIU/mL as considered diagnostic of NGGCT, since very low levels of β -HCG can be detected in germinomas. All pathological diagnosis was verified with immunohistochemical markers including placental alkaline phosphatase, AFP, β -HCG, CD117 (*c-Kit*), OCT3/4 for tumor subclassification.

A total of 110 patients were investigated. We excluded one case with final pathological diagnoses that were other than GCT, and 24 patients who did not have adequate preoperative or pretreatment MRI for evaluation. Eventually, a total of 85 patients were enrolled in the study.

MRI assessment and treatment

We analyzed the MRI features and patient information from PACS and medical charts, respectively. All MRI scans were performed on 1.5-T MRI units. The diffusion weighted imaging (DWI) parameters were as follows: TE=60–75 ms; TR=4000–5000 ms; matrix size 128×128; field of view (FOV) 300 mm; slice thickness 5 mm, voxel resolution 1.2 mm×1.2 mm×6.0 mm; and NEX 1. Diffusion was measured in three orthogonal directions by using three b-values (0, 500, and 1000 s/mm²). ADC maps were automatically calculated by the MR scanners using DWI sequences.

The MRI characteristics of tumors analyzed in the present study included the tumor location, size (max diameter), margin, cystic components, T1 hyperintense foci, enhancing patterns, intratumoral hemorrhage, quantitative ADC values, and presence of hydrocephalus. The imaging analysis was performed on the PACS workstation by consensus of two experienced qualified neuroradiologists with more than 6 years' experience of neuroradiology (CW, FC), who were blinded to the tumor histology and patient outcome. A bifocal location was defined as separate tumor involvement limited to the neurohypophyseal (sellar/suprasellar) and pineal regions on brain MR images taken at the time of diagnosis, and the presence of lesions within ventricles (including the floor of the third ventricle) was considered to represent ventricular seeding [8, 9]. Enhancing patterns were classified as no/mild enhancement and moderate/marked enhancement. The qualitative degree of contrast enhancement was defined as having all or portions of the tumor that demonstrate significantly higher signal on the postcontrast T1-weighted (T1W) images compared to

precontrast T1W images. Tumors were classified as mild enhancement when barely discernible but unequivocal degree of enhancement was present relative to pre-contrast images, and those tumors showed obvious tissue enhancement were classified as moderate/marked enhancement. Post-processing of diffusion-weighted imaging data with calculation of apparent diffusion coefficients (ADC) maps was performed by using OsiriX MD software version 7.5 (Pixmeo SARL, Switzerland) with ADC Map Calculation plugin version 1.9 (Stanford University). For each tumor, the two neuroradiologists independently determined three non-overlapped region of interest (ROI) of 20–100 mm² in the enhancing solid portion on ADC maps in conjunction with T1-weighted and post-contrast sequences. Care was taken to avoid cystic or gross hemorrhagic portions of the tumor based on T1W, T2-weighted (T2W) and T2* or EPI-T2W images. To standardize the image analysis as much as possible, the ROI was drawn on the section in which the tumor showed the enhancing solid portion with the largest diameter. In the case of multifocal or multicentric disease, the index cancer was represented by the largest volume. The pixel-by-pixel mean ADC (ADC_{mean}), minimum ADC (ADC_{min}), and maximum ADC (ADC_{max}) values for each ROI were calculated automatically by OsiriX MD software when the ROI was drawn. Then, three lesion ROIs were averaged between the two observers and used as the tumor ADC values for further analysis.

Statistical analysis

To determine independent predictors of tumor subtypes and treatment outcome, the following were assessed: gender (male vs. female), age, and MR features, including tumor location, tumor size (max diameter), tumor margin, cystic components, T1 hyperintense foci, enhancing patterns, intratumoral hemorrhage, and ADC values, and presence of obstructive hydrocephalus. Tumor subtypes were divided into two groups: (1) germinoma group and (2) NGGCT group (including teratoma, non-germinomatous GCTs and mixed germ cell tumor).

Descriptive statistics (medians and proportions) were used to characterize the clinical data, MRI features, and post-treatment status. Normality of distribution for the variables was determined by the Kolmogorov–Smirnov test. Independent *t*-tests (two-tailed) or Mann–Whitney–U-tests were used to compare continuous variable data among the groups. To test for differences in terms of dichotomous variables, Chi square tests or Fisher's exact tests (two-tailed) were used as appropriate. Receiver operating characteristic (ROC) curves analysis and area under these curves (AUC) were used to determine optimal cutoff values of ADC and to determine the potential diagnostic performance of ADC, MR features and their combination. The AUC results

greater than 0.9 was considered excellent performance, from 0.8 to 0.9 as good, from 0.7 to 0.8 as fair and lower than 0.7 as indicator of poor performance. The interobserver and intraobserver reliability of ADC value measuring was tested using intraclass correlation coefficients (ICC). All data are presented as median (range), mean \pm SD or number (percentage). All statistical analyses were performed using IBM SPSS version 22.0 (SPSS, Chicago, IL, USA), with a significance level of $P < 0.05$.

Results

Of all enrolled 85 cases, 22 were female (25.9%), and 63 were male (74.1%). The mean age of the patients at diagnosis was 11.9 (median 12.2, range 2.5–18) years. Six patients died due to tumor dissemination. The mean duration of follow-up for the remaining 79 patients was 6.3 (median 5.9, range 0.3–14.6) years. Twenty-two (25.9%) patients underwent tumor resection, 40 (47.1%) underwent biopsy, and 23 (27.1%) were diagnosed based on MRI findings, tumor marker levels, and response to radiation therapy.

In 62 patients with available histopathological data, we observed 34 germinomas, four mature teratomas, two yolk sac tumors, one choriocarcinoma and 14 mixed germ cell tumors. Of the remaining 23 patients, two patients were diagnosed with nongerminomatous germ cell tumors based on elevated serum AFP levels, and the remaining 21 patients were diagnosed with germinomas, based on their typical MR appearance, serum tumor marker levels (all without elevated serum AFP, and serum beta HCG ranging from 0.39 to 17.72 mIU/mL), and response to radiation therapy.

The mean ages at diagnosis for germinomas and NGGCTs were 11.9 ± 3.0 and 10.9 ± 4.1 years, and 11.9 ± 5.9 years for single, and multifocal GCTs, respectively, and 14.1 ± 2.6 for bifocal germinomas. There was no significant difference between the groups. Before treatment, five of 85 patients (6%) exhibited spinal seeding, while 12 of 85 (14%) exhibited ventricular seeding. At the final follow-up, 11 of 85 patients (12%) demonstrated intracranial or intra-spinal tumor recurrences.

Aside from an overall male predominance of intracranial germ cell tumors (male:female 2.5:1), there was a slight female predominance for suprasellar and double midline GCTs, with a male-to-female ratio of 0.77 (10:13) and 0.5 (2:4), respectively. A marked male predominance was also noted for GCTs in the pineal region, where the male-to-female ratio was 10.7 (32:3).

Nineteen tumors (22.4%) were located at the level of the basal ganglia, 23 (27.1%) were in the sellar/suprasellar region, 35 (41.2%) in the pineal region, six (7.1%) bifocal tumors, one (1.2%) multifocal location (in basal ganglion

and sellar/suprasellar and pineal regions) and one (1.2%) in the frontal region. All bifocal tumors were germinomas, three of which (50%) were pathologically confirmed via biopsy. For tumors in the pineal region, the incidence of initial intraventricular seeding was higher than that for other locations (28.5 vs. 4%, $P=0.001$), while the incidence of initial intraventricular seeding was lower for tumors in the sellar/suprasellar region than the remaining locations (0 vs. 19.3%, $P=0.023$).

There were significant differences in the location and histopathology of the tumors. NGGCTs were more likely to occur in the pineal region, and the case occurring in the cerebral hemispheres was an NGGCT (immature teratoma). On the other hand, all bifocal cases in the current study were germinomas, as were most sellar/suprasellar and basal ganglia GCTs. Furthermore, only four of 23 (17%) cases occurring in the sellar/suprasellar region were NGGCT.

On pre-treatment MR images, there were few significantly different MR imaging characteristics between germinomas and NGGCTs. NGGCTs (36.6 ± 17.0 mm) were significantly larger than germinomas (25.7 ± 11.6 mm; $P=0.002$). The presence of pure solid tumor (45.5 vs. 20.0%, $P=0.033$) and infiltrative margin (20.0 vs. 3.3%, $P=0.035$) were significantly more common in the germinoma than the NGGCT group. The presence of intratumoral T1 hyperintense foci (66.7 vs. 10.9%, $P<0.001$) and moderate/marked enhancement (86.7 vs. 50.9%, $P<0.001$) was significantly more common in the NGGCT group than in the germinoma group. Additionally, NGGCT was more likely to cause obstructive hydrocephalus than was germinoma (83.3 vs. 30.9%, $P<0.001$), even when the tumor was located outside pineal region (40 vs. 12.5%, $P=0.043$). On the other hand, there was no significant correlation between pre-treatment intratumoral hemorrhage and histopathological subgroups. We observed three (one germinoma and two NGGCTs) out of 85 cases (3.5%) that presented evident intratumoral hemorrhage on pre-treatment MR images based on pre- and post-contrast T1W, T2W and gradient-echo sequences. In addition, the presence of initial subependymal ventricular and/or intraspinal seeding lesions did not significantly correlate with histopathological subtypes (Figs. 1, 2).

DWI and pretreatment ADC maps were available for 61 patients with germ cell tumors. Germinoma group and NGGCT group could be differentiated from ADC_{mean} and ADC_{max} values (Fig. 3). The ADC_{mean} and ADC_{max} values ($\times 10^{-3}$ mm²/s) of solid tumor portions were significantly lower in the germinoma (1.113 ± 0.415 and 2.011 ± 0.694 , respectively) than in the NGGCT group (1.499 ± 0.469 and $2.433 \pm 0.720 \times 10^{-3}$ mm²/s; $P=0.001$ and 0.03, respectively). The ADC_{min} values were not significantly different among the groups (0.706 ± 0.355 vs. 0.781 ± 0.373 , $P=0.166$) (Table 1).

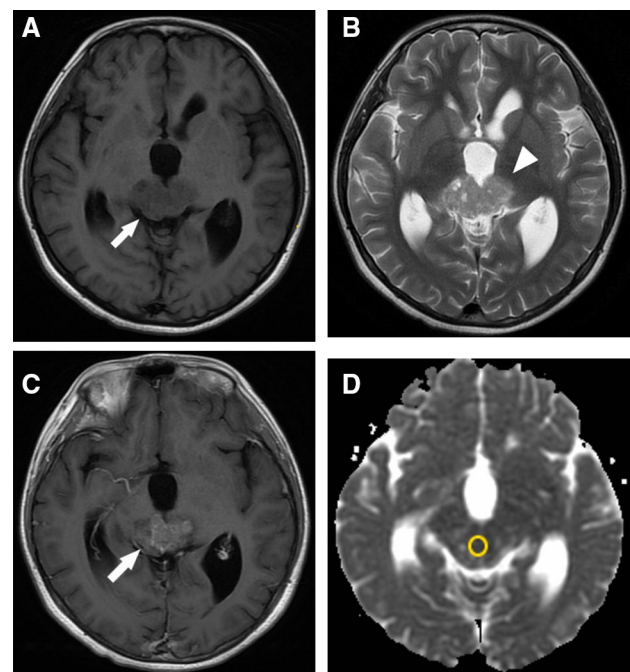


Fig. 1 A 15-year-old boy with a pineal region germinoma, proved by surgical biopsy. The tumor (arrows) is mainly hypointense without hyperintense foci on transaxial T1W (a), hyperintense on transaxial T2W (b), and heterogeneous mildly to moderately enhanced on post-contrast T1W (c) sequences (classified as moderate/marked enhancement). Transaxial T2W image also shows ill-defined margin between tumor and adjacent left thalamus is noted (arrowhead) although the margin in the right side is well-defined. Transaxial ADC map (d) demonstrates the measurement of the ADC values of the tumor with placement of a region-of-interest (ROI) on the solid portion of the tumor (circle). The mean ADC_{mean} of measurements of two radiologists is 0.832×10^{-3} mm²/s. No post-treatment intraventricular or intraspinal seeding has been noted for 5 years

By ROC analysis for each ADC-value, the cut-off value of 1.143×10^{-3} mm²/s for ADC_{mean} (ADC_{mean} threshold value) could differentiate germinoma from NGGCT with the best combination of sensitivity (71.8%) and specificity (78.3%), with a positive-predictive value (PPV) of 84.4%, and a negative-predictive value (NPV) of 62.1%, if germinoma was predicted to be lower than the threshold and NGGCT higher. According to ROC analysis, presence of intratumoral T1 hyperintense foci, ADC_{mean} threshold value, combined T1 hyperintense foci and/or ADC_{mean} threshold value, combined enhancing pattern or ADC_{mean} threshold value, and combined T1 hyperintense foci, enhancing pattern and ADC_{mean} threshold value had fair to good diagnostic performance to differentiate germinomas from NGGCT (AUC 0.735–0.809). Of all, combined lack of T1 hyperintense foci and ADC_{mean} threshold value had the highest specificity (91.3%) and PPV (92.3%), while the combination of lack of T1 hyperintense foci, no/mild enhancement and ADC_{mean} threshold value had 100% sensitivity and 100% NPV for discriminating germinoma from

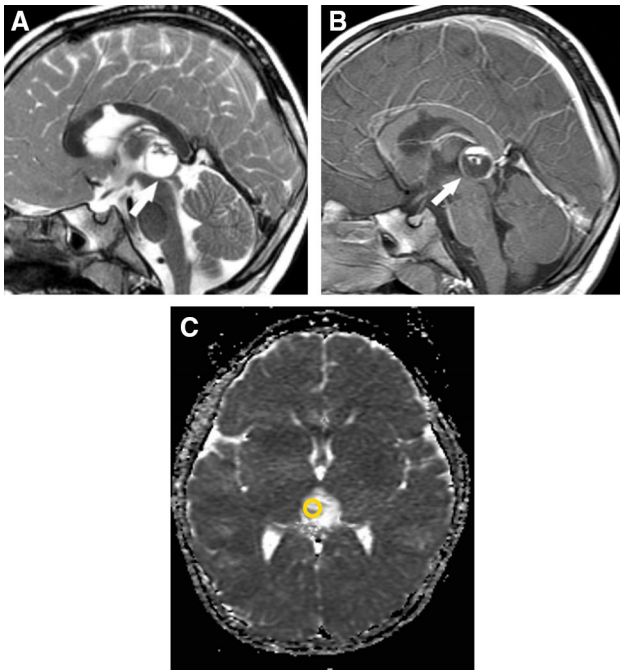


Fig. 2 A 3.5-year-old boy with a pathological-proven pineal region mature teratoma. The tumor (arrows) is mainly cystic with hyperintense on sagittal T2W (a), with moderate/well enhancement of the cystic wall and focal enhancing soft tissue inside on post-contrast T1W (b) sequences. Transaxial ADC map (c) demonstrates the measurement of the ADC values of the tumor with placement of a ROI on the solid portion of the tumor (circle). The ADC_{mean} is $1.941 \times 10^{-3} \text{ mm}^2/\text{s}$

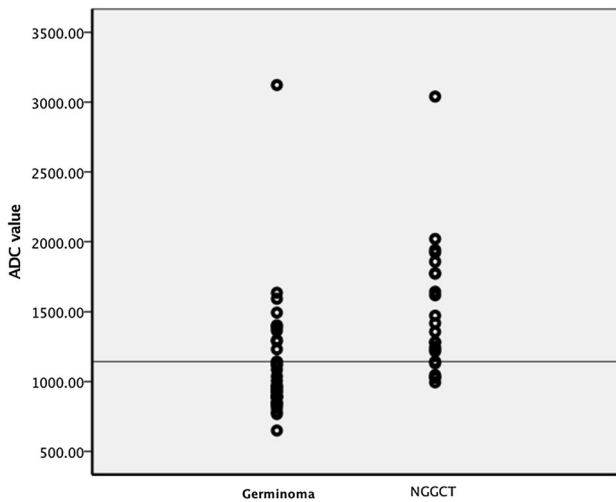


Fig. 3 Scatter diagram of average ADC_{mean} values for germinoma and nongerminomatous germ cell tumor (NGGCT). The unit of Y axis is $\times 10^{-6} \text{ mm}^2/\text{s}$. The transverse line indicates cutoff value of $1.143 \times 10^{-3} \text{ mm}^2/\text{s}$ (shown as $1143 \times 10^{-6} \text{ mm}^2/\text{s}$)

NGGCT. Table 2 shows the summary of sensitivity, specificity, PPV, NPV and AUC for MR morphological features,

ADC_{mean} , and their combination in the differentiation of germinoma from NGGCT in all patients.

The MRI features and ADC values were also expedient for distinction between germinomas and NGGCT in patients without elevated serum tumor maker, especially when used in combination. In patients with normal serum AFP and/or βhCG levels, the absence of intratumoral T1 hyperintense foci, imaging features other than cystic components with T1 hyperintense foci (morphology-1), imaging features other than cystic components with T1 hyperintense foci and moderate/marked enhancement (morphology-2), and $ADC_{mean} < 1.180 \times 10^{-3} \text{ mm}^2/\text{s}$ had fair to good diagnostic performance of differentiating germinomas from NGGCT (AUC 0.747–0.887). The combination of absent T1 hyperintense foci or morphology-1 or morphology-2 and $ADC < 1.180 \times 10^{-3} \text{ mm}^2/\text{s}$ had 100% specificity and 100% positive-predictive value (PPV) with excellent performance (AUC 0.934–0.961) in discriminating germinoma from NGGCT in this subgroup. A summary of sensitivity, specificity, PPV, NPV and AUC for MR morphological features, ADC_{mean} , and their combination in the differentiation of germinoma from NGGCT in patients with normal serum AFP and $\beta\text{-HCG}$ below 100 IU/L is shown in Table 3.

Of all the 11 cases had tumor recurrence after treatment, four were diagnosed germinomas and seven were NGGCT. Although the percentage of patients with NGGCTs who experienced post-treatment tumor recurrence was higher than that for patients with germinomas; this difference was not statistically significant ($P=0.057$). There was no significant association between tumor recurrence and gender, tumor location, MR imaging features and the extent of surgery. Interobserver reliability for of the two evaluators was very high [ICC, 0.913; 95% confidence interval (CI), 0.859–0.947; $P < 0.001$]. In the analysis of intraobserver reliability, the ICC also indicated a very high correlation of first evaluator (ICC 0.923; 95% CI 0.872–0.954; $P < 0.001$) and high correlation of second evaluator (ICC 0.887; 95% CI 0.812–0.932; $P < 0.001$).

Discussion

In Taiwan, intracranial GCTs account for 10% of pre-adult brain tumors [3]; this incidence is higher than that in Western countries, where GCTs represent only 0.5–3% of all brain tumors [5]. Intracranial GCTs include tumors with diverse histology with different tumor responses to treatment.

The distinction between germinomas and NGGCTs is important, as the extent of surgery, radiation field, and chemotherapy regimens differ between the two tumor types. However, the radiological features of intracranial

Table 1 Demographic and MR features of germinoma and NGGCT

	Germinoma	NGGCT	<i>P</i>
Gender (n)			
Male:female	38:17	23:7	0.615
Age (years) ^a	12.2 (12.2, 4.3–18)	11.4 (11.8, 2.5–16.6)	0.385
Location ^b			
Basal ganglia	15 (27.3%)	4 (13.3%)	0.536
Sellar/suprasellar	19 (34.5%)	4 (13.3%)	0.019
Pineal region	14 (25.5%)	21 (70.0%)	<0.001*
Bifocal	6 (10.9%)	0 (0%)	0.048*
Multifocal	1 (1.8%)	0 (0%)	
Lobar	0 (0%)	1 (3.3%)	
MR images			
Max diameter (mm) ^c	25.7 ± 11.69	37.4 ± 17.27.0	0.002*
Tumor component (n) (solid: cystic)	25:30	6:24	0.033*
Margin (n) (infiltrative: well defined)	11:44	1:29	0.035*
T1 hyperintense foci (n) (presence: absence)	7:48	19:11	<0.001*
Enhancement (n) (no/mild: well)	27:28	4:26	0.001*
Intratumoral bleeding (n) (presence: absence)	1:54	2:28	0.247
DWI ^c			
ADC value (×10 ⁻³ mm/s ²)	1.113 ± 0.415	1.499 ± 0.469	<0.001*
ADC _{mean}			
ADC _{max}	2.011 ± 0.694	2.433 ± 0.720	0.03*
ADC _{min}	0.706 ± 0.355	0.781 ± 0.373	0.166
Obstructive hydrocephalus			
Presence: absence	17:37	25:5	<0.001*
Initial seeding (presence: absence)			
Intraventricular seeding	10:43	2:30	0.106
Spinal seeding	2:51	3:29	0.309
Recurrent interval (years) ^c	2.2 (2.6, 0.4–3.2)	2.8 (1.1, 0.2–6.7)	0.524
Post treatment recurrence			
No recurrence ^b	49/85 (57.6%)	25/85 (29.4%)	0.0576
Presence of recurrence ^b	4 (7.3%)	7 (23.3%)	
Spinal recurrence	2	4	
Intraventricular	1	3	
Both spinal and intraventricular recurrence	1	0	

*Significance values

^aValues represent mean (median, range)^bValues represent number and percentage of patients in histologic subgroup (n, %)^cValues represent mean ± SD

GCTs are diverse among different locations and histological subgroups, although several distinct neuroimaging patterns have been reported in the literature. The early stage basal ganglia germinoma is reported to demonstrate subtle patchy/ill-defined margin T2 hyperintensity without contrast enhancement, which mimics non-tumorous condition. Albeit, the associated Wallerian degeneration and hemiatrophy of ipsilateral the brain structures are highly characteristic and reliable signs of basal ganglia germ cell tumors [8–14]. The basal ganglia germinomas are reported as isointense to hypointense on T1WI, but hyperintensity

on T1WI was also noted in early case reports [10]. In the more advanced stages, the majority of basal ganglia germinomas appear as large and heterogeneous with cystic components and enhancement. These MR features were also used as surrogates in conjunction with serum tumor makers for diagnosis in some of our cases without surgical biopsy data. Suprasellar region germinomas are reported to often have an ill-defined margin and irregular shape. On the other hand, the MRI findings of pineal region GCTs have been more widely studied, but most of them focused on the differentiation between pineal germinoma and other pineal

Table 2 Sensitivity, specificity, PPV, and NPV for MR morphology, ADC, and combined feature in the differentiation of germinomas from NGGCT (all 85 cases except ADC data was available in 61 cases)

	Sensitivity (%)	Specificity (%)	PPV (%)	NPV (%)	AUC	P
No T1 hyperintensities	88.7	62.5	79.7	76.9	0.775	0.002*
No/mild enhancement	49.1	84.4	83.9	50.0	0.650	0.051
No T1 hyperintensities AND no/mild enhancement	42.1	87.0	84.2	47.6	0.651	0.87
ADC _{mean} < 1.143 ^a	71.1	78.3	84.4	62.1	0.783	0.001*
No T1 hyperintensities OR ADC _{mean} < 1.143 ^a	71.8	19	62.2	26.7	0.749	0.005*
No T1 hyperintensities AND ADC _{mean} < 1.143 ^a	63.2	91.3	92.3	60.0	0.809	<0.001*
No/mild enhancement OR ADC < 1.143 ^a	81.6	69.6	81.6	69.6	0.772	0.002*
Combined feature	100	43.5	74.5	100	0.735	0.008*

Combined feature: other than T1 hyperintensities with well enhancement and ADC >

PPV positive predictive value, NPV negative predictive value

*Significance values

^aADC: $\times 10^{-3}$ mm²/s

Table 3 Sensitivity, specificity, PPV, and NPV for MR morphology, ADC, and their combinations in the differentiation of germinomas from NGGCT in patients with normal serum AFP and serum β -HCG below 100 IU/L

	Sensitivity (%)	Specificity (%)	PPV (%)	NPV (%)	AUC	P
No T1 hyperintense foci	55.6	88.7	45.5	92.2	0.747	0.075
Morphology-1	88.7	55.6	92.6	45.5	0.747	0.075
Morphology-2	94.3	55.6	92.6	62.5	0.774	0.049*
ADC _{mean} < 1.180 ^a	80.0	97.4	80.0	97.4	0.887	0.005*
No T1 hyperintense foci AND ADC _{mean} < 1.180 ^a	88.6	100	100	50.0	0.934	0.002*
Morphology-1 AND ADC _{mean} < 1.180 ^a	86.8	100	100	50.0	0.934	0.002*
Morphology-2 AND ADC _{mean} < 1.180 ^a	92.1	100	100	62.5	0.961	0.001*

Morphology-1: other than cystic with T1 hyperintensities

Morphology-2: other than cystic with T1 hyperintensities and well enhancement

PPV positive predictive value, NPV negative predictive value

*Significance values

^aADC: $\times 10^{-3}$ mm²/s

region tumors. Smith et al. [15] reported that presence of hyperattenuation on unenhanced CT, restriction on DWI, and isointense signal relative to gray matter on T2WI due to the high cellular nature of germinoma may aid considerably in the differentiation of GCTs from other pineal region tumors. Dumrongpisutikul et al. [16] reported a statistically significant higher mean ADC value in compared with pineal parenchymal tumors (including pineocytoma, papillary tumor of the pineal region and pineoblastoma) [16]. In a recent study, Awa et al. [17] suggested two significant imaging features differentiating germinomas from NGGCTs in the pineal region: (1) thick peritumoral edema (peritumoral T2 high signal intensity area thicker than 5 mm) and (2) bithalamic extension; however, quantitative data of ADC values were lacking in that retrospective study. In view of previous studies, data regarding MR characteristics and ADC values of intracranial non-germinomatous germ cell

tumors, particularly outside the pineal location, and the differentiation between GCT and NGGCT have been scarcely studies and are insufficient. Therefore, the main goal of the present study was to (1) characterize the imaging features that may aid in the pre-operative differentiation between germinomas and NGGCTs, and (2) to identify those factors that may increase the risk of early recurrence or that may indicate a requirement for more intensive/long-term monitoring.

Recently, epidemiological data from a large population-based tumor registry has been published for intracranial CGTs [18, 19], and our patient cohort exhibited similar patterns of distribution, including teenage onset, an overall predominance of male gender, and germinoma pathology. Additionally, all bifocal GCTs in the present study were germinomas, in agreement with the findings of previous studies, which indicates that bifocal lesions are most

frequently although not exclusively considered to be germinomas [20–24]. However, in contrast to the findings of Phi et al. [24], which indicated that bifocal GCTs were significantly associated with multifocal, disseminated disease and indicated a poor prognosis, the results of our study indicated that the presence of initial or post-treatment tumoral seeding did not significantly differ between patients with single, bifocal, or multifocal lesions. The results of the present study were comparable to those of a previous study involving a patient cohort monitored from 1989 to 2009 at our institute by Chen et al. [25], who also revealed that the number of lesions (single, multifocal, or bifocal) had no significant impact on overall survival or relapse-free survival in any of the treatment groups. When considered along with the results of these previous studies, our findings indicated that, with appropriate treatment protocols, the presence of bifocal lesions per se is not a poor prognostic sign.

In literature review, there is discrepancy of enhancing pattern of GCTs. As discussed above, early stage basal ganglia germinomas tend to show no or only subtle enhancement, while most advanced stage basal ganglia germinomas show irregular solid area with enhancement. Wang et al. [26] reported that the majority of pineal region germinoma is hypointense to isointense on T1WI, isointense to hyperintense on T2WI, with markedly homogeneous enhancement in 56 patients with intracranial germinoma and. In a review by Kakigi et al. [27] they concluded pineal germinoma shows avid enhancement which may be speckled, and NGGCTs are more likely to enhance heterogeneously in part because of hemorrhage [15]. In contrast, Dumrongpisutikul et al. [16] reported mildly enhancing (57.1%) in their pineal germinomas. In this study, the enhancing pattern was also diverse among subgroups of intracranial GCTs. Nonetheless, the combination of enhancing pattern with T1 signal intensities and ADC value serves as a better imaging indicator to distinguish germinoma from NGGCTs than using single imaging feature alone.

The role of DWI and ADC for brain tumor-typing and tumor-grading has been evaluated [28, 29]; however, the role of DWI and ADC values in assessing intracranial germ cell tumors has not been fully investigated. In our study, germinomas could be differentiated from NGGCTs using ADC_{max} values. These results are comparable to those of a recent study by Ogiwara et al., who investigated ten cases with histologically confirmed germ cell tumors. In their study, they calculated normalized ADC values as the ratio of the tumor ADC value to the control ADC, which was the average of ADC values for the normal-appearing cerebellum and bilateral centrum semiovale. The reported normalized ADC value was significantly lower for germinomas ($1.11 \pm 0.096 \times 10^{-3} \text{ mm}^2/\text{s}$) than for NGGCTs ($1.703 \pm 0.223 \times 10^{-3} \text{ mm}^2/\text{s}$; $P=0.01$) [7]. These results

are comparable to those of the present study, although the definite values are different, which may be due to different methods for placement used for ROI placement and choice of ADC values. ADC values in brain tumors are inversely related to cellularity and the ratio of the nuclear area to cytoplasm. In NGGCTs, particularly in yolk sac tumors and immature teratomas, the tumor cells are not as densely packed, and cellularity is not markedly high, as compared to classic germinomas. This characteristic hypercellularity of germinomas is considered to result in lower ADC values in germinomas than in NGGCTs. Although the presence of hyperintense foci representing fat or calcified components within the tumor may indicate NGGCTs, the sensitivity of this characterization approach is low in patients without elevated tumor markers, probably because the calcifications in some tumors in the NGGCT group are indistinguishable from pineal calcifications engulfed by a germinoma. In addition, basal ganglia germinomas are reported to show high signal intensity on T1WI without enhancement in the early stage [11, 12, 14, 30]. Furthermore, intratumoral hemorrhage, which is not uncommon in intracranial GCTs [5, 8, 12, 14], also leads to the presence of T1 hyperintensities. Our study indicates that combined MR features, using a lack of T1 hyperintensities and ADC_{mean} values less than $1.143 \times 10^{-3} \text{ mm}^2/\text{s}$ can increase the specificity and PPV in diagnosis of germinoma overall. Moreover, the combination of T1 hyperintense foci, an enhancing pattern and an ADC_{mean} value with a cutoff value of $\times 1.180 \times 10^{-3} \text{ mm}^2/\text{s}$ can serve as an imaging marker with 100% specificity and 100% PPV in cases with normal serum AFP and serum beta-HCG below 100 IU/L. Such differentiation may be applied in future planning of surgical as well as non-surgical treatment.

In the present study, we were interested in determining whether a clinical or MR feature could be used as a marker of increased recurrence risk. However, we were unable to identify any factor as a significant predictor of tumor recurrence, possibly because the overall case number was small, and also the numbers of recurrent and deceased cases observed were too small to be statistically meaningful. Furthermore, case excluded from the current cohort was controversial. The excluded case had one well-defined non-enhancing lesion in the sellar to suprasellar region, with isointense on both T1W and T2W images with clinical presentation of central diabetes insipidus. He received surgical resection due to partially tumor regression after radiotherapy and the histopathological result revealed a Rathke's cleft cyst. Whether this was a rare case of mixed Rathke's cleft cyst and germinoma which responded to radiation, or whether it was a true false-positive diagnosis of germinoma, it is necessary to recognize the radiological pitfalls and diagnostic limitations in order to minimize the impact on image interpretation and improve patient care.

Although serum and CSF tumor markers are mandatory for making a diagnosis, and neurosurgery/histological confirmation is generally necessary for diagnosis in patients without elevated beta-HCG, the cut-off values for elevated beta-HCG vary between institutes and study groups (from 50 mIU/mL in the Children's Oncology Group study ACNS0232, to 50–100 mIU/mL in the ACNS1123 study). The contribution of surgery to a superior treatment outcome, when given before or after radiotherapy combined with chemotherapy, is still debated. For tumors in critical and/or deep locations, such as the basal ganglia and pineal region, where gross total resection may be difficult, tissue biopsy could pose the risk of inadequate sampling or under-representation of the histological components of the entire tumor [30]. An extensive review of the literature by Balossier et al. [31] has shown that tissue diagnosis is less accurate with endoscopic procedures than with stereotactic procedures (81.1 vs. 93.7%) for pineal tumor biopsies. In addition, the optimal selection of biopsy sites for bifocal lesions is unclear, and whether the benefit of biopsy at both sites outweighs the adverse effects of these difficult procedures remains to be determined. There is also a possible risk of sampling error when sampling a single lesion in a bifocal germ cell tumor. In our study, the results of combined MR features could aid differentiation of the germinoma group from the NGGCT group in patients with or without tumor marker elevation. It has a potential clinical role when deciding on whether to perform a biopsy in patients with tumors in critical locations, selecting the target site in bifocal lesions, and considering a second-look surgery in the context of dubious histological results in terms of clinical conditions and MR features.

The present study had some limitations. Radiological interpretations of ADC measurements may vary considerably. However, we attempted to minimize such variation via accurate placement of ROIs sampling the enhanced solid portion of the tumor. Furthermore, although the overall number of patients with available DWI was fairly large as compared to previous studies, the number of patients with tumor recurrence or who had died was rather small. Additionally, due to the retrospective nature of the study, potential selection bias existed and the results of MR spectroscopy and MR perfusion were lacking. Nonetheless, our results should be interpreted with caution due to the limited number of patients studied. Our findings should be verified by further studies involving larger cohorts of patients.

Conclusion

MRI features, including tumor size, location, T1 hyperintense foci, intratumoral cystic components, tumor margin, enhancing pattern, and ADC_{mean} values of intracranial

germ cell tumors may facilitate preoperative differentiation of intracranial germinoma from NGGCTs, especially by using a combination of T1 hyperintense foci and/or enhancing pattern with ADC. Such differentiation may apply in planning of surgical as well as non-operative treatment.

References

1. Ho DM, Liu HC (1992) Primary intracranial germ cell tumor. Pathologic study of 51 patients. *Cancer* 70:1577–1584
2. Matsutani M, Sano K, Takakura K, Fujimaki T, Nakamura O, Funata N, Seto T (1997) Primary intracranial germ cell tumors: a clinical analysis of 153 histologically verified cases. *J Neurosurg* 86:446–455. doi:10.3171/jns.1997.86.3.0446
3. Wong TT, Ho DM, Chang KP, Yen SH, Guo WY, Chang FC, Liang ML, Pan HC, Chung WY (2005) Primary pediatric brain tumors: statistics of Taipei VGH, Taiwan (1975–2004). *Cancer* 104:2156–2167. doi:10.1002/cncr.21430
4. Matsutani M (2004) Clinical management of primary central nervous system germ cell tumors. *Semin Oncol* 31:676–683
5. Echevarria ME, Fangusaro J, Goldman S (2008) Pediatric central nervous system germ cell tumors: a review. *Oncologist* 13:690–699. doi:10.1634/theoncologist.2008-0037
6. Yen SH, Chen YW, Huang PI, Wong TT, Ho DM, Chang KP, Liang ML, Chiou SH, Lee YY, Chen HH (2010) Optimal treatment for intracranial germinoma: can we lower radiation dose without chemotherapy? *Int J Radiat Oncol Biol Phys* 77:980–987. doi:10.1016/j.ijrobp.2009.06.035
7. Ogiwara H, Tsutsumi Y, Matsuoka K, Kiyotani C, Terashima K, Morota N (2015) Apparent diffusion coefficient of intracranial germ cell tumors. *J Neurooncol* 121:565–571. doi:10.1007/s11060-014-1668-y
8. Moon WK, Chang KH, Kim IO, Han MH, Choi CG, Suh DC, Yoo SJ, Han MC (1994) Germinomas of the basal ganglia and thalamus: MR findings and a comparison between MR and CT. *AJR Am J Roentgenol* 162:1413–1417. doi:10.2214/ajr.162.6.8192009
9. Kim DI, Yoon PH, Ryu YH, Jeon P, Hwang GJ (1998) MRI of germinomas arising from the basal ganglia and thalamus. *Neuroradiology* 40:507–511
10. Okamoto K, Ito J, Ishikawa K, Morii K, Yamada M, Takahashi N, Tokiguchi S, Furusawa T, Sakai K (2002) Atrophy of the basal ganglia as the initial diagnostic sign of germinoma in the basal ganglia. *Neuroradiology* 44:389–394. doi:10.1007/s00234-001-0735-1
11. Oyama N, Terae S, Saitoh S, Sudoh A, Sawamura Y, Miyasaka K (2005) Bilateral germinoma involving the basal ganglia and cerebral white matter. *AJNR Am J Neuroradiol* 26:1166–1169
12. Phi JH, Cho BK, Kim SK, Paeng JC, Kim IO, Kim IH, Kim DG, Jung HW, Kim JE, Wang KC (2010) Germinomas in the basal ganglia: magnetic resonance imaging classification and the prognosis. *J Neurooncol* 99:227–236. doi:10.1007/s11060-010-0119-7
13. Rasalkar DD, Chu WC, Cheng FW, Paunipagar BK, Shing MK, Li CK (2010) Atypical location of germinoma in basal ganglia in adolescents: radiological features and treatment outcomes. *Br J Radiol* 83:261–267. doi:10.1259/bjr/25001856
14. Lee SM, Kim IO, Choi YH, Cheon JE, Kim WS, Cho HH, You SK (2016) Early imaging findings in germ cell tumors arising from the basal ganglia. *Pediatr Radiol* 46:719–726. doi:10.1007/s00247-016-3542-x
15. Smith AB, Rushing EJ, Smirniotopoulos JG (2010) From the archives of the AFIP: lesions of the pineal region:

- radiologic-pathologic correlation. *Radiographics* 30:2001–2020. doi:[10.1148/rg.307105131](https://doi.org/10.1148/rg.307105131)
16. Dumrongpisutikul N, Intrapromkul J, Yousem DM (2012) Distinguishing between germinomas and pineal cell tumors on MR imaging. *AJNR Am J Neuroradiol* 33:550–555. doi:[10.3174/ajnr.A2806](https://doi.org/10.3174/ajnr.A2806)
 17. Awa R, Campos F, Arita K, Sugiyama K, Tominaga A, Kurisu K, Yamasaki F, Karki P, Tokimura H, Fukukura Y, Fujii Y, Hanaya R, Oyoshi T, Hirano H (2014) Neuroimaging diagnosis of pineal region tumors—quest for pathognomonic finding of germinoma. *Neuroradiology* 56:525–534. doi:[10.1007/s00234-014-1369-4](https://doi.org/10.1007/s00234-014-1369-4)
 18. Goodwin TL, Sainani K, Fisher PG (2009) Incidence patterns of central nervous system germ cell tumors: a SEER Study. *J Pediatr Hematol Oncol* 31:541–544. doi:[10.1097/MPH.0b013e3181983af5](https://doi.org/10.1097/MPH.0b013e3181983af5)
 19. Villano JL, Virk IY, Ramirez V, Propp JM, Engelhard HH, McCarthy BJ (2010) Descriptive epidemiology of central nervous system germ cell tumors: nonpineal analysis. *Neuro-oncol* 12:257–264. doi:[10.1093/neuonc/nop029](https://doi.org/10.1093/neuonc/nop029)
 20. Sugiyama K, Uozumi T, Arita K, Kiya K, Kurisu K, Sumida M, Harada K (1994) Clinical evaluation of 33 patients with histologically verified germinoma. *Surg Neurol* 42:200–210
 21. Lafay-Cousin L, Millar BA, Mabbott D, Spiegler B, Drake J, Bartels U, Huang A, Bouffet E (2006) Limited-field radiation for bifocal germinoma. *Int J Radiat Oncol Biol Phys* 65:486–492. doi:[10.1016/j.ijrobp.2005.12.011](https://doi.org/10.1016/j.ijrobp.2005.12.011)
 22. Cuccia V, Alderete D (2010) Suprasellar/pineal bifocal germ cell tumors. *Child's Nerv Syst* 26:1043–1049. doi:[10.1007/s00381-010-1120-3](https://doi.org/10.1007/s00381-010-1120-3)
 23. Aizer AA, Sethi RV, Hedley-Whyte ET, Ebb D, Tarbell NJ, Yock TI, Macdonald SM (2013) Bifocal intracranial tumors of nongerminomatous germ cell etiology: diagnostic and therapeutic implications. *Neuro-oncol* 15:955–960. doi:[10.1093/neuonc/not050](https://doi.org/10.1093/neuonc/not050)
 24. Phi JH, Kim SK, Lee J, Park CK, Kim IH, Ahn HS, Shin HY, Kim IO, Jung HW, Kim DG, Paek SH, Wang KC (2013) The enigma of bifocal germ cell tumors in the suprasellar and pineal regions: synchronous lesions or metastasis? *J Neurosurg Pediatr* 11:107–114. doi:[10.3171/2012.10.PEDS11487](https://doi.org/10.3171/2012.10.PEDS11487)
 25. Chen YW, Huang PI, Ho DM, Hu YW, Chang KP, Chiou SH, Guo WY, Chang FC, Liang ML, Lee YY, Chen HH, Hsu TR, Lin SC, Wong TT, Yen SH (2012) Change in treatment strategy for intracranial germinoma: long-term follow-up experience at a single institute. *Cancer* 118:2752–2762. doi:[10.1002/ncr.26564](https://doi.org/10.1002/ncr.26564)
 26. Wang Y, Zou L, Gao B (2010) Intracranial germinoma: clinical and MRI findings in 56 patients. *Child's Nerv Syst* 26:1773–1777. doi:[10.1007/s00381-010-1247-2](https://doi.org/10.1007/s00381-010-1247-2)
 27. Kakigi T, Okada T, Kanagaki M, Yamamoto A, Fushimi Y, Sakamoto R, Arakawa Y, Mikami Y, Shimono T, Takahashi JC, Togashi K (2014) Quantitative imaging values of CT, MR, and FDG-PET to differentiate pineal parenchymal tumors and germinomas: are they useful? *Neuroradiology* 56:297–303. doi:[10.1007/s00234-014-1334-2](https://doi.org/10.1007/s00234-014-1334-2)
 28. Wu CC, Guo WY, Chen MH, Ho DM, Hung AS, Chung HW (2012) Direct measurement of the signal intensity of diffusion-weighted magnetic resonance imaging for preoperative grading and treatment guidance for brain gliomas. *J Chin Med Assoc* 75:581–588. doi:[10.1016/j.jcma.2012.08.019](https://doi.org/10.1016/j.jcma.2012.08.019)
 29. Kinoshita Y, Yamasaki F, Tominaga A, Ohtaki M, Usui S, Arita K, Sugiyama K, Kurisu K (2016) Diffusion-weighted imaging and the apparent diffusion coefficient on 3 T MR imaging in the differentiation of craniopharyngiomas and germ cell tumors. *Neurosurg Rev* 39: 207–213; discussion 213. doi:[10.1007/s10143-015-0660-0](https://doi.org/10.1007/s10143-015-0660-0)
 30. Takeuchi S, Takasato Y (2011) Can stereotactic sample biopsies accurately diagnose mixed germ cell tumors? *Acta Neurochir* 153: 1535; author reply 1537–1538. doi:[10.1007/s00701-011-1032-3](https://doi.org/10.1007/s00701-011-1032-3)
 31. Balossier A, Blond S, Touzet G, Lefranc M, de Saint-Denis T, Maurage CA, Reyns N (2015) Endoscopic versus stereotactic procedure for pineal tumour biopsies: comparative review of the literature and learning from a 25-year experience. *Neurochirurgie* 61:146–154. doi:[10.1016/j.neuchi.2014.06.002](https://doi.org/10.1016/j.neuchi.2014.06.002)